# Al-$\sqrt{3}\times\sqrt{3}$ domain structure on Si(111)-7×7 observed by scanning tunneling microscopy

Katsuya Takaoka, Masamichi Yoshimura, and Takafumi Yao
*Department of Electrical Engineering, Hiroshima University, Kagamiyama, Higashi-hiroshima 724, Japan*

Tomoshige Sato, Takashi Sueyoshi, and Masashi Iwatsuki
*JEOL Ltd., Akishima, Tokyo 196, Japan*

(Received 17 November 1992; revised manuscript received 11 May 1993)

Scanning tunneling microscopy is used to study the structure of Al-$\sqrt{3}\times\sqrt{3}$ domains on the Si(111)-7×7 surface and the atomic arrangement around the domain boundary. Al-$\sqrt{3}\times\sqrt{3}$ domains grow from kink sites of the ⟨110⟩ or ⟨211⟩ step and extend over the Si-7×7 terrace. Detailed investigation around the boundaries reveals that faulted sites face the boundaries on the Si-7×7 side, while on the Al-$\sqrt{3}\times\sqrt{3}$ side, Al adatoms occupy the $T_4$ sites except on the rows adjacent to the phase boundaries where Al (or Si) atoms are adsorbed on the Si adatom sites. The latter atoms play an important role in retaining the dimer structure at the boundaries.

The atomic and electronic structure of metal overlayers on semiconductor surfaces have been widely studied in order to understand metal-semiconductor interfaces. Among the ordered metal-overlayer systems observed, the most well known is the Si(111)-$\sqrt{3}\times\sqrt{3}R30°$ reconstruction appearing at $\frac{1}{3}$ monolayer (ML) coverage.[1–4] Al induces a $\sqrt{3}\times\sqrt{3}$ reconstruction. With respect to the adsorption site, two different types of symmetrical sites on Si(111) can be considered; one is the $H_3$ site where Al atoms adsorb above the Si atoms in the fourth layer and the other is the $T_4$ site above the second-layer Si atoms. Northrup examined these two adatom models using the first-principles pseudopotential calculation of the total energy and of the surface state dispersion,[5] and concluded that the $T_4$ model was more favorable. Qualitative support to this assignment was later given by means of angle-resolved ultraviolet photoelectron spectroscopy (ARUPS),[6] low-energy electron diffraction (LEED),[7] and $k$-resolved inverse-photoemission spectroscopy (KRIPES).[8] Recently, Hamers and Demuth reported that the tunneling spectroscopy measurement on the Al-$\sqrt{3}\times\sqrt{3}$ structure indicates that the $T_4$ site is preferred over the $H_3$ site.[9,10] However, the local atomic structure at the phase boundary between the Si-7×7 domain and the Al-$\sqrt{3}\times\sqrt{3}$ domain at low Al coverage has not been understood yet.

In this paper, we report the scanning tunneling microscopy (STM) results on the coexisting area of Si-7×7 and Al-$\sqrt{3}\times\sqrt{3}$ and discuss the local atomic structure at the phase boundary. It is found that the Si-7×7 structure holds a dominant position on the upper region of ⟨110⟩ or ⟨211⟩ step edges and Al-$\sqrt{3}\times\sqrt{3}$ structure on the lower region, indicating that the Al-$\sqrt{3}\times\sqrt{3}$ domains grow from the step and extend over the terrace. Detailed investigation on the phase boundary confirms that the faulted halves of the 7×7 unit cells are faced to the boundary, on the other side, Al atoms occupy the $T_4$ sites except adjacent rows to the boundary where Al (or Si) atoms occupy on the Si adatom positions. The important role of the latter Al (or Si) atoms is presented.

The STM used in this study is a commercial UHV-STM (JEOL JSTM-4000XV) capable of high-temperature operation. $N$-type, $P$-doped Si(111) with resistivity of 1–10 Ω cm was used as a substrate. After introducing into the STM chamber, the base pressure of which is below $1.8\times10^{-9}$ Pa, the substrate was outgassed overnight. The surface was cleaned by repetitive thermal annealing at 1200 °C for a few seconds, which yielded a large flat area of 7×7 reconstruction. In order to obtain, coexisted areas of 7×7 and Al-$\sqrt{3}\times\sqrt{3}$, Al of less than $\frac{1}{3}$ monolayer coverage was deposited with use of a tungsten basket onto the substrate at room temperature followed by annealing at 580 °C. Alternatively, Al was deposited onto the heated substrate at 550 °C. STM measurements were performed at room temperature or during heating the sample. An electrolytically polished tungsten tip was used to probe tunneling current.

Figure 1 shows an STM image of Al-adsorbed surfaces after the deposition of less than $\frac{1}{3}$ ML at room temperature. Al atoms adsorbs as clusters on the Si(111)-7×7

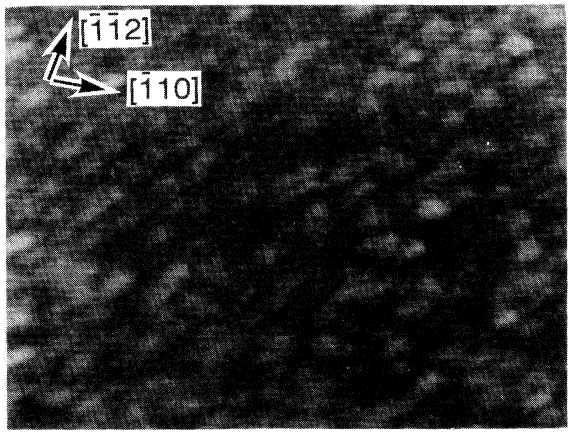


FIG. 1. STM current image of Al clusters deposited on the Si(111)-7×7 at room temperature ($V_s$=2 V, $I_{av}$=0.08 nA, 38×30 nm$^2$).

 

clean surface. No preferable adsorption site in the 7×7 unit cells was recognized, which was in contrast to Cu or Ag on Si(111).[11] The sample was then annealed at 580 °C for 10 s and cooled down to room temperature. Figure 2 shows a 100×80 nm$^2$ image taken with the sample bias of 1.72 V and the average tunneling current ($I_{av}$) of 0.4 nA. Si-7×7 and Al-$\sqrt{3}\times\sqrt{3}$ domains coexist on each terrace with atomic steps along the ⟨110⟩ or ⟨211⟩ direction. It is noted that the 7×7 domain situates on the upper region of the step edges and the $\sqrt{3}\times\sqrt{3}$ domain on the lower region. The $\sqrt{3}\times\sqrt{3}$ domain does not exist as islands on the terrace but contacts step edges. The same spatial distribution of the $\sqrt{3}\times\sqrt{3}$ and 7×7 domains was observed on the surface prepared by depositing not only Al of less than $\frac{1}{3}$ ML onto a heated substrate, but a few monolayers of Al onto the substrate followed by annealing. In the latter case the coexisting area is considered to be formed by desorption of Al atoms from the Al-$\sqrt{3}\times\sqrt{3}$ surface. These facts indicate that the step sites play an important role to form the $\sqrt{3}\times\sqrt{3}$ domain on the 7×7 surface or vice versa: The Al-$\sqrt{3}\times\sqrt{3}$ domain grows from the lower sites of the steps to take over the 7×7 terrace and Al atoms desorb from the upper sites of the steps.

Figure 3(a) shows a high-temperature (600 °C) STM image of a phase boundary between the Si-7×7 and Al-$\sqrt{3}\times\sqrt{3}$. The upper and lower parts of the figure represent the 7×7 and Al-$\sqrt{3}\times\sqrt{3}$ domains, respectively. Figure 3(b) shows a schematic view of atomic positions observed in a part of Fig. 3(a), in which Al positions based on the $T_4$ (indicated by triangles) and $H_3$ (indicated by squares) models are superimposed. On the Si-7×7 side, the faulted sites are observed to face the boundary. This is due to the fact that more energy is necessary to form the $\sqrt{3}\times\sqrt{3}$ atomic arrangement on the faulted site which contains the stacking fault layer than on the unfaulted site, since in order to form the $\sqrt{3}\times\sqrt{3}$ atomic arrangement, the stacking fault should be rearranged. The observed Al adsorption sites, indicated by closed circles, are in good agreement with the $T_4$ sites except for those adjacent to the boundary. It is noted here that though we cannot determine whether the atoms adjacent to the boundary are Al or Si, we hereafter tentatively assign them to Al since Al is considered to be energetically favorable rather than Si judging from the absence of dangling bonds. This assignment does not essentially affect the following discussion. The Al adatoms adjacent to the boundary are found to occupy not the $T_4$ sites but the Si adatom positions of the 7×7 unit cell. The former and the latter Al atoms are referred to $N$ and $A$ atoms hereaf-

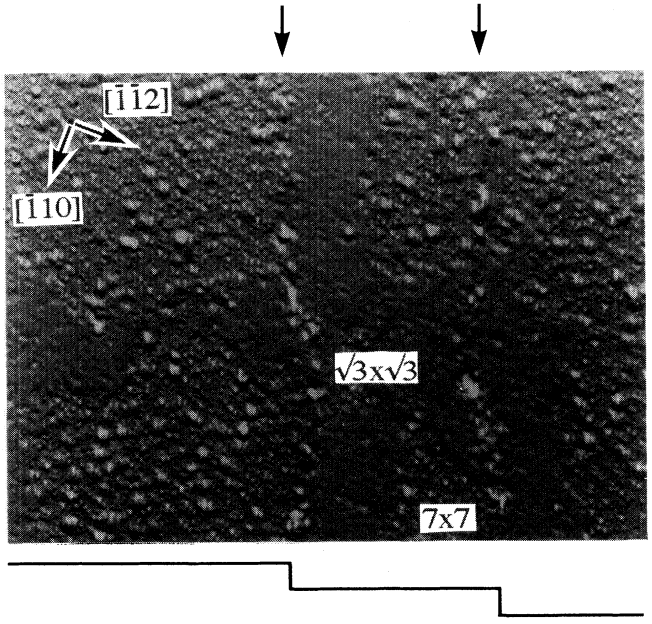


FIG. 2. STM current image showing a coexisting area of 7×7 and Al-$\sqrt{3}\times\sqrt{3}$ structures taken at room temperature ($V_s$=1.72 V, $I_{av}$=0.4 nA, 100×80 nm$^2$). The 7×7 structure holds a dominant position on the upper region of step edges and the $\sqrt{3}\times\sqrt{3}$ structure on the lower region.

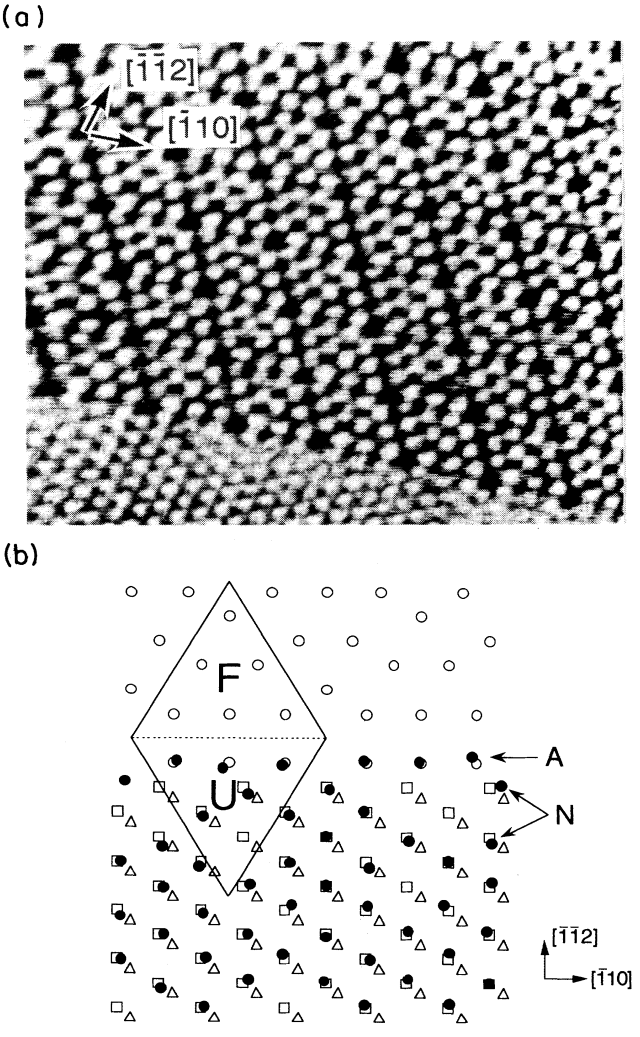


FIG. 3. (a) STM current image at around a domain boundary between the Si-7×7 and Al-$\sqrt{3}\times\sqrt{3}$ taken at 600 °C ($V_s$=−0.18 V, $I_{av}$=0.5 nA, 18×16 nm$^2$). (b) A schematic representation of (a) superimposed on possible models (□, $T_4$ site; △, $H_3$ site; ○, Si adatom site; ●, experiment).

ter. In order to understand why the $A$ atoms should appear at the boundary, a comparison is carried out between the boundary structure based on the atomic arrangement observed experimentally (model $a$) and the reference structure where all Al atoms adsorb on the $T_4$ sites (model $b$). Figure 4 shows schematics of simple bonding configurations of models $a$ and $b$. The $7\times7$ unfaulted half site and the $\sqrt{3}\times\sqrt{3}$ unit cell are drawn in the solid lines for reference. In model $a$, three bonds from the $A$ atom (hatched circles) is completed by bonding the three Si atoms underneath for simplicity. In the 21 times periodicity along the $\langle 110\rangle$ direction indicated by the dashed line, the number of dangling bonds of Si and Al in model $a$ is 10 and 6, while in model $b$ it is 12 and 2, respectively. Judging from the total number of the dangling bonds, model $a$ seems energetically less favorable. Therefore, the difference in the configuration of Al dangling bonds should be taken into account. Al dangling bonds appear at the nearest sites of the $A$ atoms in model $a$, while they are located at the boundary in model $b$. In model $a$ the Al dangling bond of $N$ can be shared with the nearest Si atom which bonds to an $A$ atom, while in model $b$ it would be implausible because available Si atoms are located at the next-nearest position. In addition, the more Si dangling bonds are situated at the boundary, the less stable the dimer structure at the boundary becomes. Therefore, the Al adatoms favor the Si adatom positions at the boundary. When the dimer row is broken and the stacking fault layer is rearranged, the Al domain can extend over the unfaulted site and pass easily onto an adjacent unfaulted site until it reaches a phase boundary with a faulted site. Thus, the $A$ atoms should exist at the domain boundary to keep the Si domain stable.

When the sample is repetitively annealed at higher temperature up to 900 °C and is quenched, the Al-$\sqrt{3}\times\sqrt{3}$ structure is observed with many defects at around the boundary, as shown in Fig. 5(a). The temperature of 900 °C is high enough to induce not only the phase transition between the Si-$7\times7$ and the Si-$1\times1$ but also the desorption of Al. Therefore, it is likely that the surface annealed at such a high temperature becomes defective after quenching in contrast to the surface in Fig. 3(a). A detailed study of the defects observed will be reported elsewhere. Figure 5(b) shows a schematic of the atomic positions observed in a part of Fig. 5(a). It should be noted that all of $A$ atoms are still observed after higher-temperature annealing. The double positionings of Al atoms on the $T_4$ sites are indicated by cross-hatched circles. This rearrangement seems to be caused by the displacement of Al atoms from the normal positions as indicated by arrows. When the double positioning occurs, the number of dangling bonds from the $A$ atoms at the boundary decreases though the total number of them increases. It is again emphasized that the $A$ atoms are very important to maintain the dimer row to keep the phase boundary.

In conclusion, the STM observations of the domain distribution of the Al-$\sqrt{3}\times\sqrt{3}$ structure on Si(111)-$7\times7$ after the adsorption or desorption of Al demonstrate that the $\sqrt{3}\times\sqrt{3}$ domains form at the lower region of step

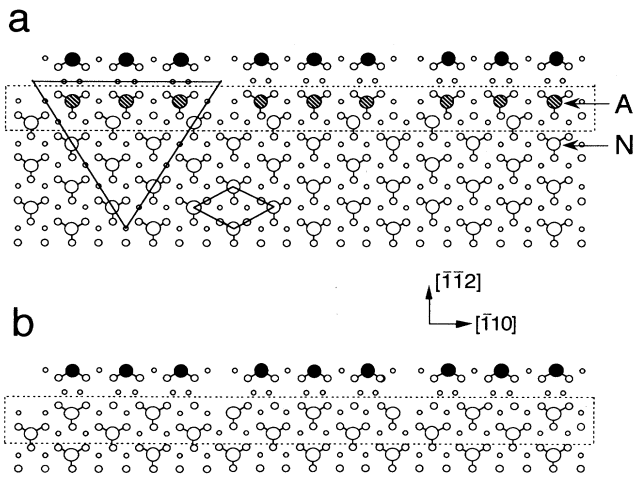


FIG. 4. Possible structural models of a domain boundary between the $7\times7$ and $\sqrt{3}\times\sqrt{3}$ phases. Model $a$ is based on the experimental results: Al atoms adsorb on the $T_4$ sites ($N$ atoms) except the adjacent rows where they adsorb on the Si adatom sites of $7\times7$ reconstruction ($A$ atoms). Model $b$: all Al adatoms adsorb on the $T_4$ sites.

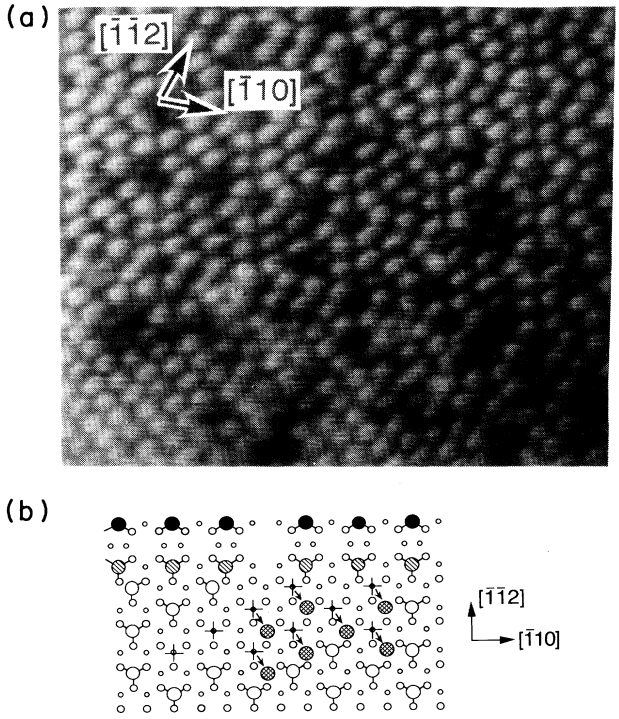


FIG. 5. (a) STM topographic image at a domain boundary taken at room temperature after higher-temperature annealing up to 900 °C ($V_s=1$ V, $I=0.3$ nA, $17\times13$ nm$^2$). (b) A schematic representation of Fig. 4(a). Open, hatched, and cross-hatched circles indicate Al atoms experimentally observed in the $T_4$ position, in the Si-$7\times7$ adatom position, and in another $T_4$ position (double positioning), respectively, while crosses indicate a point defect in the $T_4$ position.

edges and extend over the 7×7 terrace, and desorbs at the upper region of the step edges to form Si-7×7. Close STM images at around the domain boundary between the Si-7×7 and Al-$\sqrt{3}\times\sqrt{3}$ reveal that the faulted sites of the 7×7 unit cells are faced to the boundary and that Al adatoms are found to occupy the $T_4$ site except for Al (or Si) adatoms adjacent to the boundary which are situated on the Si adatoms position of the 7×7 unit cell. The latter atoms have an important role to retain dimer rows for keeping the domain boundaries stable. When the sample is annealed at higher temperature (900 °C), there appear many point defects including surface vacancies and double positioning on the $T_4$ sites. However, $A$ atoms are still situated on the Si adatom positions at the phase boundary.

The authors are grateful to A. Kawazu and H. Sakama of the University of Tokyo for valuable comments.

[1]J. J. Lander and J. Morrison, Surf. Sci. **2**, 553 (1964).
[2]G. Margaritondo, J. E. Rowe, and S. B. Christman, Phys. Rev. B **14**, 5396 (1976).
[3]G. V. Hansson, R. Z. Bachrach, R. S. Bauer, and P. Chiaradia, Phys. Rev. Lett. **46**, 1033 (1981).
[4]H. Nagayoshi, Solid State Sci. **59**, 167 (1985).
[5]J. E. Northrup, Phys. Rev. Lett. **53**, 683 (1984).
[6]R. I. G. Uhrberg, G. V. Hasson, J. M. Nicholls, and P. E. S. Persson, Phys. Rev. B **31**, 3805 (1985).
[7]H. Huang, S. Y. Tong, W. S. Yang, H. D. Shih, and F. Jona, Phys. Rev. B **42**, 7483 (1990).
[8]J. M. Nicholls, B. Reihl, and J. E. Northrup, Phys. Rev. B **35**, 4137 (1987).
[9]R. J. Hamers and J. E. Demuth, J. Vac. Sci. Technol. A **6**, 512 (1988).
[10]R. J. Hamers, Phys. Rev. B **40**, 1657 (1989).
[11]St. Tosch and H. Neddermeyer, Phys. Rev. Lett. **61**, 349 (1988).

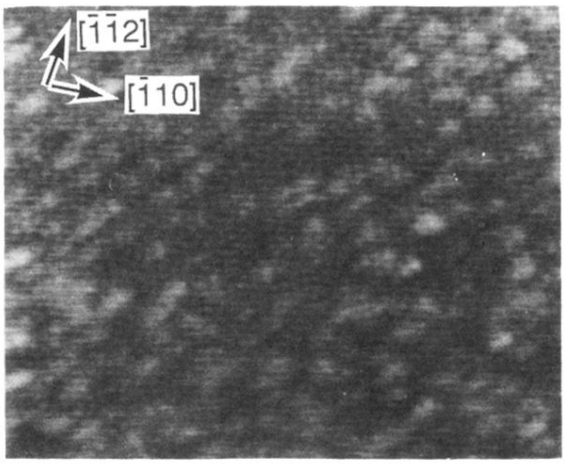


FIG. 1. STM current image of Al clusters deposited on the Si(111)-7×7 at room temperature ($V_s$=2 V, $I_{av}$=0.08 nA, 38×30 nm$^2$).

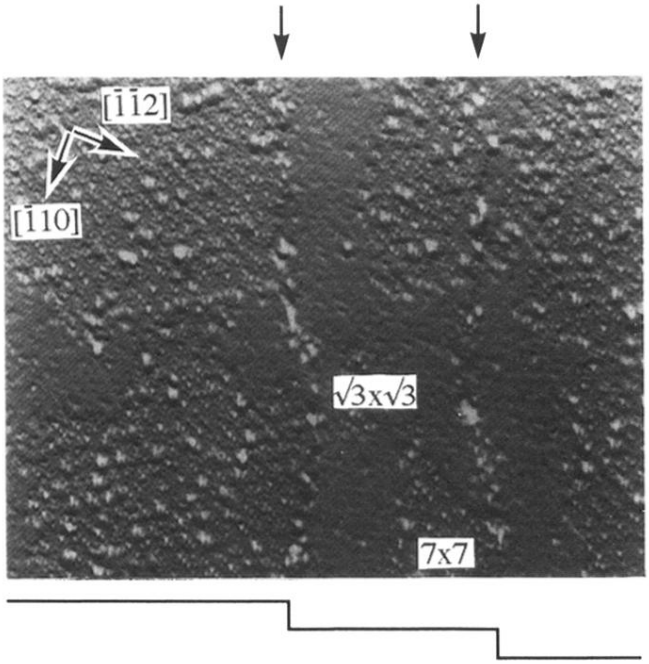


FIG. 2. STM current image showing a coexisting area of $7\times7$ and Al-$\sqrt{3}\times\sqrt{3}$ structures taken at room temperature ($V_s=1.72$ V, $I_{av}=0.4$ nA, $100\times80$ nm$^2$). The $7\times7$ structure holds a dominant position on the upper region of step edges and the $\sqrt{3}\times\sqrt{3}$ structure on the lower region.

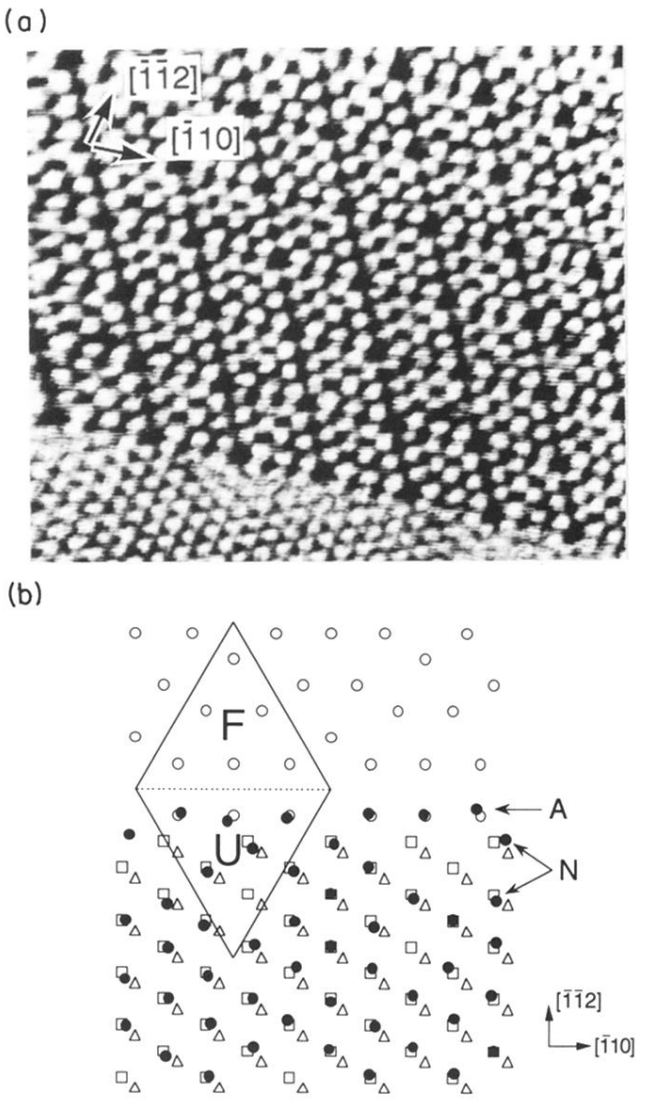


FIG. 3. (a) STM current image at around a domain boundary between the Si-7×7 and Al-$\sqrt{3}\times\sqrt{3}$ taken at 600 °C ($V_s = -0.18$ V, $I_{av} = 0.5$ nA, $18\times16$ nm$^2$). (b) A schematic representation of (a) superimposed on possible models (□, $T_4$ site; △, $H_3$ site; ○, Si adatom site; ●, experiment).

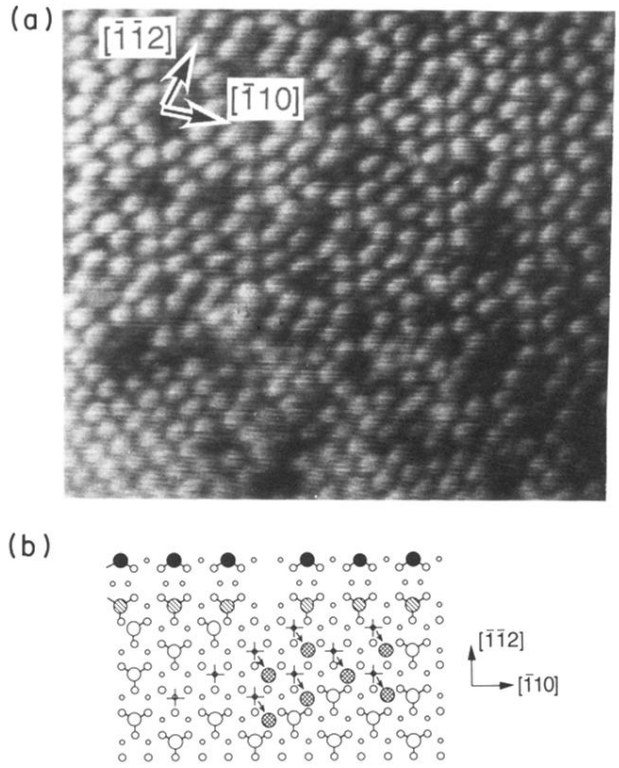


FIG. 5. (a) STM topographic image at a domain boundary taken at room temperature after higher-temperature annealing up to 900 °C ($V_s = 1$ V, $I = 0.3$ nA, $17 \times 13$ nm$^2$). (b) A schematic representation of Fig. 4(a). Open, hatched, and cross-hatched circles indicate Al atoms experimentally observed in the $T_4$ position, in the Si-7×7 adatom position, and in another $T_4$ position (double positioning), respectively, while crosses indicate a point defect in the $T_4$ position.